Fabrication of polyimide based microfluidic channels for biosensor devices

Zulfiqar, Azeem; Pfreundt, Andrea; Svendsen, Winnie Edith; Dimaki, Maria

Published in:
Journal of Micromechanics and Microengineering

Link to article, DOI:
10.1088/0960-1317/25/3/035022

Publication date:
2015

Document Version
Publisher's PDF, also known as Version of record

Fabrication of polyimide based microfluidic channels for biosensor devices

2015 J. Micromech. Microeng. 25 035022

(http://iopscience.iop.org/0960-1317/25/3/035022)

OPEN ACCESS
IOP Publishing
Journal of Micromechanics and Microengineering
J. Micromech. Microeng. **25** (2015) 035022 (8pp)
doi:10.1088/0960-1317/25/3/035022

Fabrication of polyimide based microfluidic channels for biosensor devices

Azeem Zulfiqar, Andrea Pfreundt, Winnie Edith Svendsen and Maria Dimaki

Department of Micro- and Nanotechnology, Technical University of Denmark, Ørsteds Plads, Building 345B, DK - 2800 Kgs. Lyngby, Denmark

E-mail: maria.dimaki@nanotech.dtu.dk

Received 15 October 2014, revised 2 December 2014
Accepted for publication 16 December 2014
Published 11 February 2015

Abstract

The ever-increasing complexity of the fabrication process of Point-of-care (POC) devices, due to high demand of functional versatility, compact size and ease-of-use, emphasizes the need of multifunctional materials that can be used to simplify this process. Polymers, currently in use for the fabrication of the often needed microfluidic channels, have limitations in terms of their physicochemical properties. Therefore, the use of a multipurpose biocompatible material with better resistance to the chemical, thermal and electrical environment, along with capability of forming closed channel microfluidics is inevitable. This paper demonstrates a novel technique of fabricating microfluidic devices using polyimide (PI) which fulfills the aforementioned properties criteria. A fabrication process to pattern microfluidic channels, using partially cured PI, has been developed by using a dry etching method. The etching parameters are optimized and compared to those used for fully cured PI. Moreover, the formation of closed microfluidic channel on wafer level by bonding two partially cured PI layers or a partially cured PI to glass with high bond strength has been demonstrated. The reproducibility in uniformity of PI is also compared to the most commonly used SU8 polymer, which is a near UV sensitive epoxy resin. The potential applications of PI processing are POC and biosensor devices integrated with microelectronics.

Keywords: closed channel microfluidics, polyimide process, polyimide to polyimide bonding

(Some figures may appear in colour only in the online journal)

1. Introduction

Microfluidic channels are key components in point-of-care (POC) and biosensor devices. Recent developments in the field of microfluidics have changed their role from mere source of transferring fluid samples within the device to more diverse purposes, like blood sample handling, where capillary forces along with the Dean force can separate blood plasma and serum within the microfluidic channel [1], functionalization of biosensors for specific biomolecule detection, functionalized silicon nanowire based sensors with closed channel microfluidic systems [2] and measurement of specific protein concentration in the solution by label-free impedance bead-based assays [3]. This advancement in the field of microfluidics has led to the need of a multipurpose material that can provide a platform for microfluidics and has the capability to integrate it with CMOS based electrical read-out systems often used in POC devices. A material with a simple fabrication process, which is resistant to various harsh chemicals, stable at higher temperatures, and has good electrical passivation properties and biocompatibility is often desirable in this respect. The most commonly used materials for microfluidic channels now-a-days such as SU8, PDMS (poly-dimethyl siloxane), PMMA (poly-methylmethacrylate) and COP (cyclic olefin copolymer) have their limitations in one or more of the aforementioned properties. For example formation of SU-8

structures involves complex fabrication process steps and their optimization, i.e. soft baking, UV exposure, post exposure baking, development and final baking. A slight change in any of the fabrication process steps can result in delamination, cracking and bad resolution [4]. Similarly, PDMS and PMMA are not chemically resistant against many organic solvents used in microelectronics fabrication [5], which can be a hurdle in the process integration of microfluidics with microelectronics to produce POC devices.

Polyimide (PI) with its high resistance against many chemicals, high glass transition temperature, high dielectric constant and biocompatibility [6] is an emerging candidate material for microfluidics based devices as an alternative to the most commonly used ones. The etch rate of PI in hydrofluoric acid (HF) and buffered hydrofluoric acid (BHF), which are commonly used chemicals in silicon based biosensor devices, is very low, at around 5 nm min^{-1} [7]. The glass transition temperature of around 325 °C enables PI to withstand most of the microelectronics packaging techniques like wire bonding, flip chip bonding etc. The dielectric constant of around 3.4 (at 1 kHz and room temperature) is quite close to silicon dioxide SiO_2 (3.9 at 1 kHz and room temperature) [8] which qualifies PI to be used as passivation layer for microelectronic circuit in the POC and biosensor devices.

In recent years, PI has been one of the main areas of research for microfluidics devices. Several PI based microfluidic devices have been demonstrated using different methods. Metz *et al* [9] have developed a process to fabricate flexible devices using photosensitive PI, where the PI with microstructures is bonded to another PI followed by their release from the carrier substrates. They have implemented this technique on manufacturing an implantable, flexible polyimide probe with microelectrodes and microfluidic channels for simultaneous drug delivery and multi-channel monitoring of bioelectric activity [10]. Their process is however limited to creating only up to 5–20 μm high structures. Moreover the structures shrink when fully cured and the channels do not have vertical sidewalls. Both of these phenomena can create problems in microfluidic applications, where precision and predictability of the flows is important. Youn *et al* [11] have demonstrated the formation of microfluidic channels in a PI film by hot embossing using a silicon master mold. This process creates well defined channels but issues with reusability of the mold arise as in other hot embossing applications. On the other hand, Nguyen *et al* [12] have studied the etching parameters of non-photosensitive PI to obtain deep anisotropic microfluidic channels. They have taken a sheet of PI and used a Nickel / Chromium mask to etch it deep with silicon dioxide as a stopping layer. Although they demonstrate the use of PI sheets as gaskets for sealing microfluidic systems, the process is limited to the creation of through holes. This was also the focus of the work of Mimoun *et al* [13] but again no data of the applicability of the method for creating other structures is shown. Other works focus on etching fully cured PI [14] and present etching parameters but for thicknesses not necessarily relevant for microfluidics applications. Finally, Bayrashev *et al* [15] have studied the PI–PI bonding by using RF dielectric heating to develop a new wafer bonding technique, achieving bond strength of more than 1.5 MPa for non-photosensitive PI. As bonding is very important when creating microfluidic channels in order to achieve good sealing, it is essential to develop a technique to achieve this that can easily be integrated with the remaining microfabrication steps.

As PI is still in the developing phase and has not replaced the commonly used materials for microfluidics completely, some of its properties, that might be utilized to develop POC and biosensors devices with integrated microfluidics channels, remain unexplored.

In this paper, the material properties of non-photosensitive PI are exploited to develop a simple fabrication process for microfluidic devices of various dimensions. More specifically, partially cured PI is investigated, as opposed to fully cured PI, that can achieve strong PI–PI and PI–glass bonding and is applicable in closed channel microfluidics for biosensors. A detailed study of the etching parameters for partially cured PI (not fully imidized/polymerized) using a reactive ion etcher (RIE) and an inductively coupled plasma (ICP) etcher with silicon nitride Si_3N_4 and aluminum Al mask is presented. The optimized etching recipes are also compared with those for fully cured PI. The capabilities of this polymer are also investigated in terms of reproducibility in the processing of the layers. Moreover, bonding parameters for PI–PI and PI–glass bonding are developed followed by the bond strength tests using pressure drop measurements.

2. Materials and methods

Non-photosensitive PI-2574 supplied by HD Microsystems™ was selected for the experiments due to its good adherence to substrates like quartz, pyrex and silicon, and its self-priming capability that allows multi-coating. The fabrication of microfluidic channels in PI was done on a quartz wafer and two methods for patterning PI were developed, one by using a plasma enhanced chemical vapor deposition (PECVD) Si_3N_4 mask and one by using an Al mask. The two fabrication processes are described in detail below.

2.1. Fabrication using Si_3N_4 mask

Step 1: 10 μm PI-2574 was spin coated over a 4 inch quartz wafer at 2400 rpm for 30 s with 100 rpm s^{-1} ramp rate followed by soft bake in the hotplate at 120 °C for 5 min. For >10 μm thick PI, the coating and soft baking steps were repeated as mentioned above. Every further coating step gave around 10 μm additional thickness of PI over the substrate. The final curing was done for 1 h at 300 °C.

Step 2: Deposition of 120 nm PECVD Si_3N_4 using STS Mesc Multiplex CVD system was done at 300 °C.

Step 3: 1.5 μm AZ5214e photoresist was patterned by photolithography.

Step 4: PECVD Si_3N_4 was etched using STS MESC Multiplex ICP system and photoresist was stripped-off for 5 min in rough acetone bath and 10 min in fine acetone bath with ultrasound.

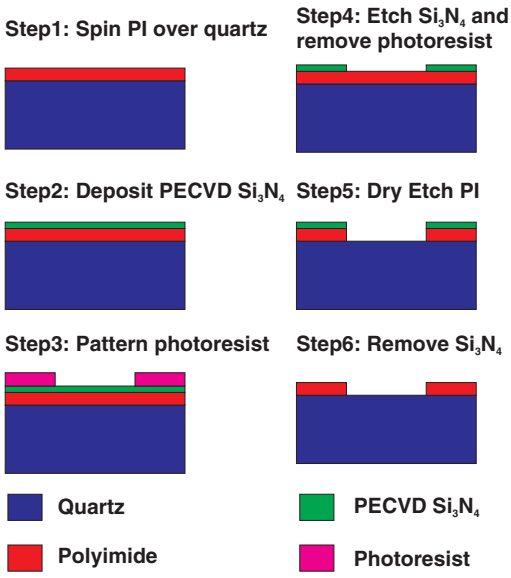

Figure 1. Schematic images of fabrication steps to pattern PI using Si_3N_4 mask.

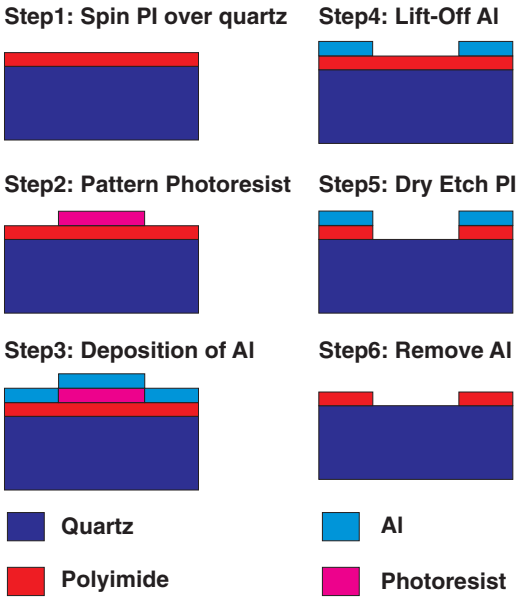

Figure 2. Schematic images of fabrication steps to pattern PI using Al mask.

Step 5: PI was etched by using RIE STS Cluster System C010 and ICP STS MESC Multiplex etching. In the ICP system the chuck temperature was set to −20 °C and the wafer was electrostatically clamped. To enable a better electrostatic clamping in ICP, we deposited Al on the back side of the quartz wafer with e-beam evaporation. In RIE there is no option for setting the chuck temperature and no clamping method is applied in the machine, therefore no Al was deposited on the back.

Step 6: As a last step, the Si_3N_4 mask is removed by wet etching in BHF for 2 min.

The schematic diagrams of all the fabrication steps are shown in figure 1.

2.2. Fabrication using Al mask

Step 1: Same as for the Si_3N_4 process but the final curing was done for 1 h at 250 °C.

Step 2: 1.5 μm AZ5214e photoresist was spin coated and patterned by photolithography followed by descuming in the plasma asher for 3 min to make the surface rougher for better adhesion of Al

Step 3: Al was deposited by an e-beam evaporation method using Alcatel SCM 600 E-beam and sputtering deposition system.

Step 4: Lift-off of Al in acetone for 30 min with ultrasonic stirring.

Step 5: Same as for the Si_3N_4 process.

Step 6: The Al was removed by dipping the whole wafer in MF-322 developer. The fabrication steps for this method are depicted schematically in figure 2.

2.3. Etching of PI

The optimization of the etching parameters for PI in the RIE and ICP systems was done by changing the pressure, RF power, gas flows and gas mixture (O_2 and Ar, and O_2 and CF_4/SF_6) in the chamber. The starting parameters were chosen as previously described in [12, 16, 17]. The etching of PI with Si_3N_4 mask was only done with O_2 and Ar mixture whereas etching with Al mask was done with O_2 and CF_4/SF_6 mixture. The reason for choosing Al mask was that fluorine based gases attack the Si_3N_4 mask, which can disappear in longer etching times.

2.4. Comparison of PI and SU8 reproducibility

3 wafers of 30 μm high microfluidic channels were made in PI using the multi coating method described above and the process reproducibility in terms of achieved channel height was compared to that of channels made by SU8 fabricated using a previously described method [4] with a slight modification i.e. the second step of spin coating speed was changed from 4000 to 3000 rpm to achieve the height of 30 μm. The height measurements were done using a profilometer (Dektak XTA by Veeco) on all the wafers and the standard deviation was calculated. The uniformity of the coatings was also checked around 5 points in the wafer: center, right edge, left edge, top edge and bottom edge.

2.5. PI–PI and PI–glass bonding

The wafers produced by Al mask were not fully cured and were used for PI–PI and PI–glass bonding experiments. The bottom wafer used for both PI–PI and PI–glass bonding had PI microfluidic channels made by the fabrication steps explained in figure 2 and the top glass wafer was covered with partially cured PI without any microfluidic channels for PI–PI bonding and without PI for PI–glass bonding experiments. Holes were milled on the top wafer using a diamond-coated drill forming inlet and outlet holes to enable fluid flow through

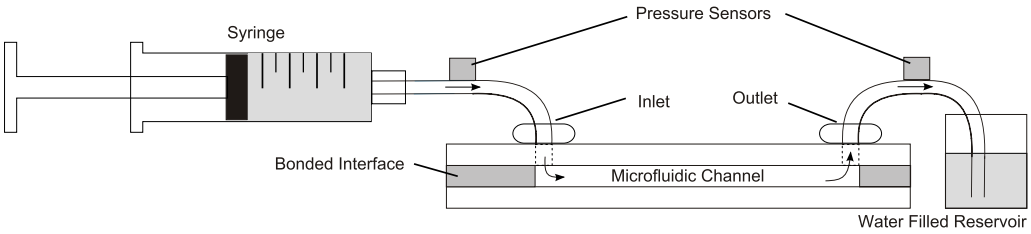

Figure 3. Schematic diagram of the setup used to perform pressure drop measurements.

the microfluidic channel. The bonding was done using an EV Group Bond aligner 610 in vacuum at 300 °C. The force and the time of bonding were varied to obtain optimal bonding. The force applied during the bonding was varied from 12 to 15 kN and the time period was varied from 15 to 30 min.

2.6. Pressure drop measurement

To evaluate possible deformation of the channel after bonding the microfluidic resistance was measured after dicing both PI–PI and PI–glass bonded wafers. The pressure drop across devices with a microfluidic channel with the dimensions Length × Width × Height = 3118 × 77 × 22.9 μm for PI–PI and Length × Width × Height = 3118 × 77 × 11.6 μm for PI–glass bonded devices was measured at different flow-rates (0.001–0.8 ml min^{-1}). Two gauge pressure sensors (Honeywell, 24PCGFH1G) were flush mounted at the in- and outlet of the device as shown in figure 3. For readout the sensors were connected to a DAQ card and a LabVIEW program. A Keithley sourcemeter was used for excitation at a fixed voltage of 10 V. The given linear range of the pressure sensors reaches up to 250 psi/17.2 bar corresponding to roughly 140 mV output voltage. Calibration of the sensors was confirmed using a compressed air source with an external gauge pressure sensor. The output voltages of both sensors were recorded simultaneously during each flow measurement and left to stabilize for a few minutes. Pressure differences were calculated from the recorded data, plotted and fitted using MATLAB.

3. Results

3.1. Etch rate characterization using Si_3N_4 mask

PI was etched in the presence of 98% O_2 and 2% Ar, and the highest etch rate was achieved with the ICP system, at 1 μm min^{-1} compared to an etch rate of 0.5 μm min^{-1} using the RIE system. The etch rate for RIE and ICP system was further characterized by studying its change with varying power which was found to be linear for the experimental parameters tested, as shown in figure 4.

Using this combination of gases in both RIE and ICP for etching, grass-like residues were observed in the bottom of the microfluidic channel. These residues were removed when a mixture of O_2 and CF_4 was used in RIE to etch the last 1 μm of PI. Figure 5(*a*) shows the SEM images of residues in the channel and in 5(*b*) the channel is free from residues.

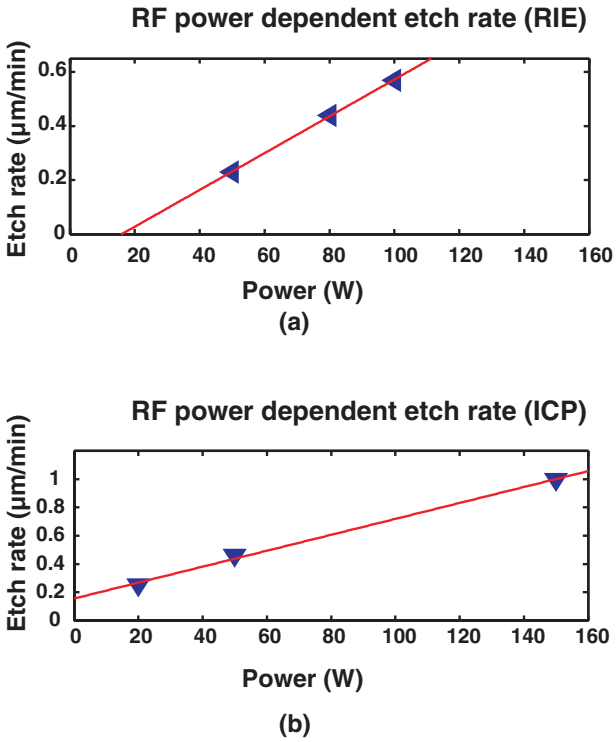

Figure 4. Etch rate of partially cured PI as a function of power in the chamber using Si_3N_4 mask. (*a*) In RIE the pressure of the chamber is 200 mTorr and the ratio of O_2/Ar is 98/2 (*b*) In ICP the pressure of the chamber is 80 mTorr, the ratio of O_2/Ar is 98/2 and Coil power is 2000 W

3.2. Etch rate characterization using Al mask

Partially cured PI was used with Al mask. It was etched by using 94% O_2 with 6% CF_4 in RIE and 80% O_2 with 20% SF_6 mixture in ICP as the CF_4 gas was not available and low gas flows were not stable in the ICP system. The etch rate was characterized by changing pressure, power, gas flow and the ratio of gases in the chamber. Figure 6 shows an increase in the etch rate in both systems by increasing the RF power and platen power respectively while keeping the pressure constant at 200 mTorr in RIE and 50 mTorr in ICP. It was observed that there is a linear relationship between the power in the chamber and the etch rate.

The pressure in the chamber is related linearly to the etch rate in the ICP system whereas this is not the case in RIE. Figure 7 shows the graphical representation of the etch rate in both systems. The RF power was kept constant at 20 W in RIE and for ICP the platen power was kept constant at 200 W.

It was also observed that the etch rate was independent of the total gas flow, if the ratio of gases in the mixture remained

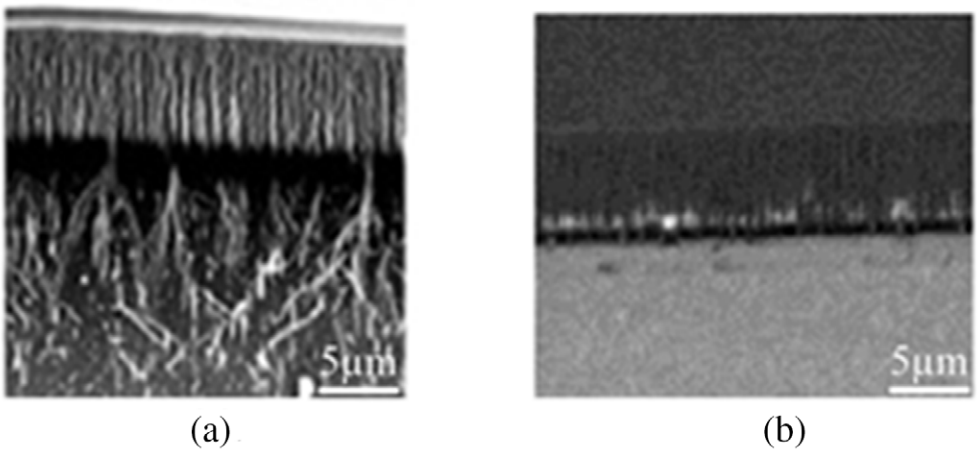

Figure 5. SEM images after etching of Polyimide using Si_3N_4 mask in RIE (*a*) Residues are visible if CF_4 is not used at all for etching PI (*b*) No residues are visible if the last 1 μm of PI is etched with mixture of O_2 and CF_4.

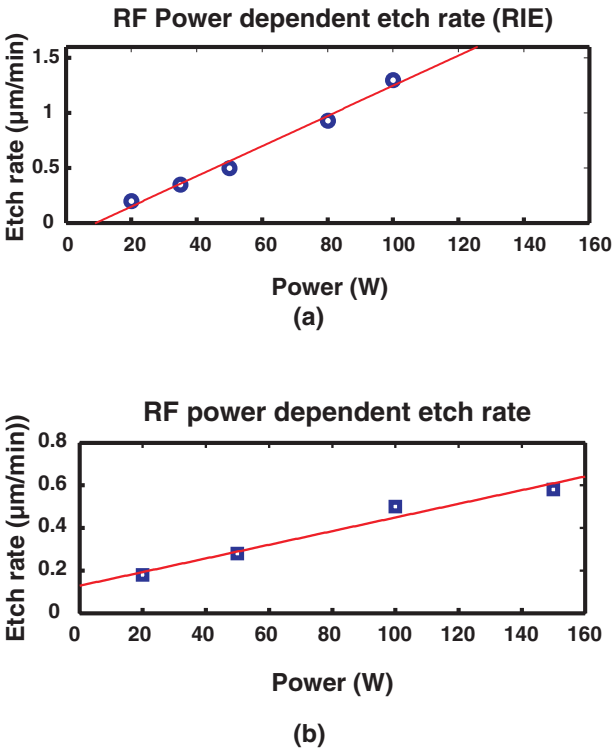

Figure 6. Etch rate of partially cured PI as a function of power in the chamber using Al mask (*a*) The pressure of the chamber is 200 mTorr and the ratio of O_2/CF_4 is 94/6 in RIE (*b*) the pressure of the chamber is 50 mTorr, the ratio of O_2/SF_6 is 80/20 and Coil power is 2000 W in ICP.

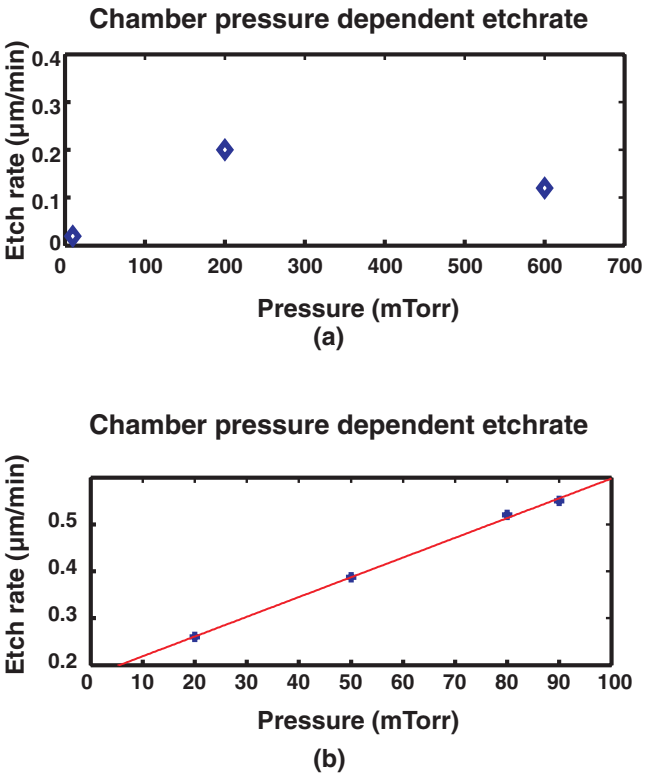

Figure 7. Etch rate for partially cured PI as a function of pressure in the chamber (*a*) the RF power is 20 W and the ratio of O_2/CF_4 is 85/15 in RIE (*b*) the platen power is 200 W, the ratio of O_2/SF_6 is 80/20 and Coil power is 2000 W in ICP.

constant, i.e. changing the total gas flow (O_2 + CF_4) in RIE from 100 to 116 sccm and (O_2 + SF_6) in ICP from 100 to 124 sccm while keeping the ratio of gases constant in both cases, did not affect the etch rate.

Once the etching parameters were defined for partially cured PI, the same recipe of RIE system was applied on fully cured PI i.e. cured at 350 °C for 1 h, to determine if it was applicable to both. It was found that the etch rate was low when the ratio of O_2/CF_4 (94/6) used for partially cured PI was applied to it.

The optimal etch rate was obtained by using O_2/CF_4 in 80/20 ratio, as shown in table 1.

3.3. Reproducibility

The five point profilometer measurements of height of the channels were done on the wafers with PI and SU8 to establish and compare the uniformity and reproducibility. The standard deviation values for both polymers were calculated for each wafer and are shown in table 2. It can be observed

Table 1. Parameters used to etch partially cured PI are different from fully cured PI.

	Pressure (mTorr)	Power (W)	Gas flow (sccm)		Etch rate μm min^{-1}
			O_2	CF_4	
Partially cured PI	200	100	94	6	1.3
Fully cured PI	200	100	94	6	0.55
Fully cured PI	200	100	80	20	0.9

The change in the ratio of O_2/CF_4 changes the etch rate by almost two fold.

Table 2. Mean thickness measurements of channel's height along with standard deviation for each wafer made from SU8 and PI.

Wafer number	SU8 mean thickness + standard deviation (μm)	PI mean thickness + standard deviation (μm)
W1	32.988 + 1.24	31.38 + 0.513
W2	34.35 + 1.285	31.29 + 0.352
W3	34.606 + 1.54	31.48 + 0.396

that the variation in the thickness on the PI wafers is smaller than for the SU8 wafers both on a wafer level but also between different wafers.

3.4. PI–PI and PI–glass bonding

PI to PI/glass bonding parameters at wafer level were also optimized. A nice homogeneous bonding was found with 15 kN force and 15 min bonding time in both cases. A quick leakage test was done after the bonding for a qualitative estimate of the bonding and no leakage was observed, indicating that integrity of bonding was maintained throughout the length of the channel. An SEM image of the channel cross section in the case of PI to glass bonding is shown in figure 8.

3.5. Pressure drop measurements

The pressure drop across the device for different flow rates shows a linear behavior within the tested pressure range up to approximately 15 bars for both PI–PI (*a*) and PI–glass (*b*) bonded chips as shown in figure 9. This shows that there is no deformation or delamination of the bonded channel with increasing pressure, which would most likely result in a change in hydraulic resistance and thus a deviation from the linear curve. The experimentally determined resistance of the channel (tubing and in- outlet resistance can be neglected) is $1.96\ 10^{14}\,\mathrm{Pa \cdot s\,(m^3 \cdot s)^{-1}}$ for the PI–Glass bonded device and $4.89\ 10^{13}\,\mathrm{Pa \cdot s\,m^{-3}}$ for the larger PI–PI bonded channel. Comparing these with the calculated values using the Hagen–Poiseuille law for a rectangular channel given in table 3 shows a very good agreement for the PI–PI bonded device. Considering the much smaller height and the accuracy in the measurement of the dimensions the values for the PI-glass bonded device are also within the expected range.

4. Discussion

In this paper, we have developed and demonstrated a simple method to produce PI based microfluidic devices by exploiting its properties and using partially cured PI as key component. Etching parameters for partially cured PI were defined and the patterning method was simplified, by using an Al mask for etching PI that can easily be dissolved from the PI surface with the help of MF-322 developer after etching without damaging the device.

The partially cured PI showed different etch rate behaviour compared to fully cured PI that is commonly used in microfluidic devices. The initial etching parameters to etch the partially cured PI were taken from previously reported work [12, 16, 17], where a detailed study had been done to achieve higher etch rates in fully cured PI using a mixture of oxygen and fluorine based gases in the plasma with minimum under etch. The technique was optimized here for partially cured PI followed by characterization of the etch rate by changing parameters such as gases, power applied and pressure in the chamber.

In order to improve the etch rate of partially cured PI both RIE and ICP etching systems were used, which rely on different etching principles. Using a Si_3N_4 mask, where only O_2 and Ar were used to etch PI, the highest etch rate of around 1.34 μm was achieved in ICP for an O_2/Ar gas flow of 98/2 sccm, chamber pressure of 80 mTorr, platen power of 150 W and coil power of 2000 W. This high etch rate is due to high density of ions applied using coil power in ICP system which is in agreement with previously published work by [13] for fully cured PI. However, by this method grass like residues are formed at the bottom of the channel in the end of the process. The grass-like residues have a silicon rich ingredient which comes from the fact that PI-2574 contains a silane (a-aminopropyl-triethoxysilane) based adhesion promoter which enhances its self-priming capability to the wafer surface and also enables multi-coating [13]. In addition to this, we claim that at a thickness higher than 10 μm, O_2 plasma cannot generate enough reactive sites by ion bombardment to completely break the PI chains and thus non-volatile components are created, which are the source of residues [18]. The addition of fluorine by using CF_4/SF_6 gas in mixture with O_2 not only helps in attacking Si containing ingredients but also helps in creating more reactive sites in PI and thus reduces the activation energy, which results in a cleaner surface in the end. For PI thickness under 10 μm, the residue problem can be overcome by etching the last 1 μm with a mixture of O_2 and CF_4/SF_6 but this is not the case for a PI thickness larger than 10 μm because etching without the presence of fluorine based gases heats up the substrate and the longer etching time results in the burning of residues which are then impossible to remove. Moreover, the mixture of O_2 and CF_4/SF_6 attacks the Si_3N_4 mask and should therefore be avoided for longer etching times.

The above limitations were overcome by replacing Si_3N_4 by Al as a masking material due to its strong resistance against fluorine based gases as compared to Si_3N_4, which allowed us to use a mixture of O_2 and CF_4/SF_6 for etching PI for the entire etch duration. Our results indicate that the etch rate of PI increases by increasing the RF power and platen power in RIE and ICP respectively. The high power induces more ions in

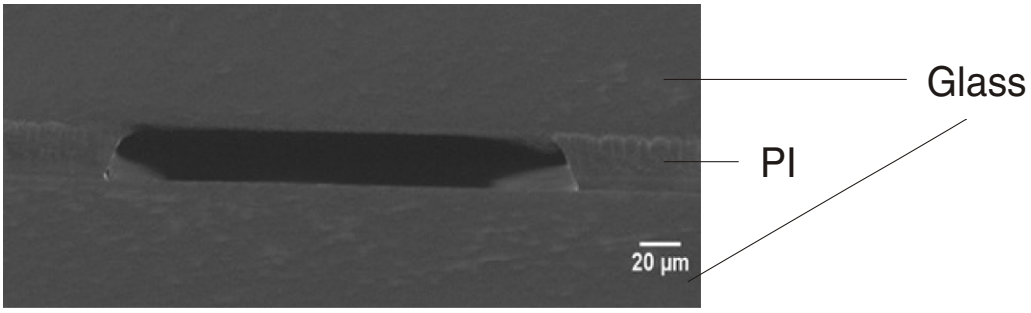

Figure 8. SEM image of the cross-section of the closed-microfluidic channel formed by PI–glass bonding.

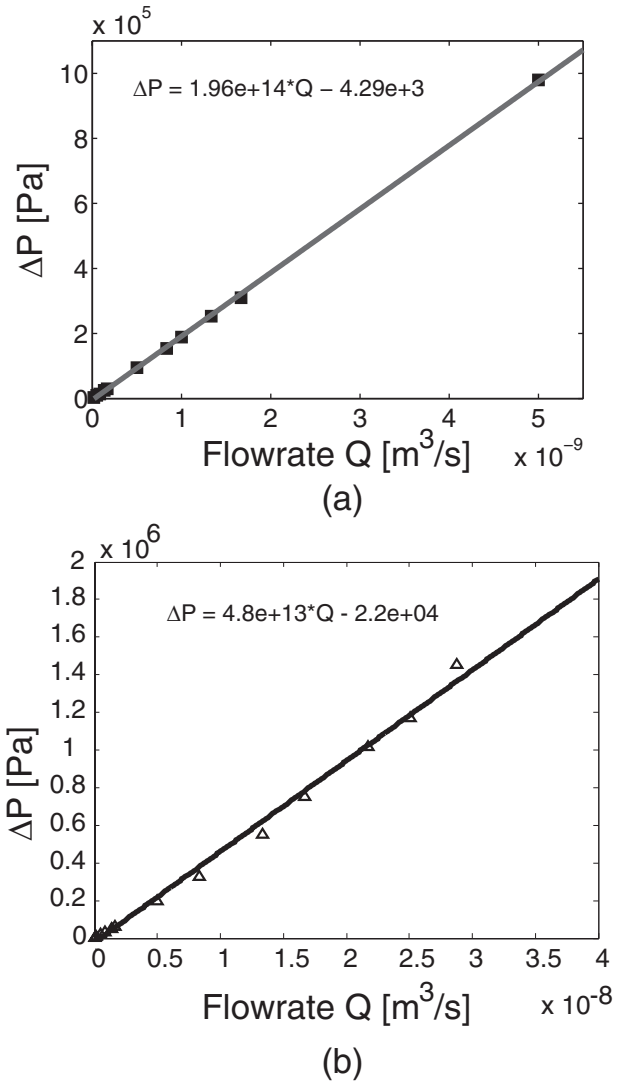

Figure 9. Pressure drop test after bonding (*a*) PI–PI bonded microfluidic channel with dimensions Length × Width × Height = 3118 × 77 × 22.9 μm (*b*) PI–glass bonded microfluidic channel with dimensions Length × Width × Height = 3118 × 77 × 11.6 μm.

the plasma that help in breaking the chains in the PI, but at the same time the substrate is heated due to higher number of ions bombarding the substrate [13, 16, 18, 19]. This overheating of the substrate enables the carbonization of the polyimide and starts producing grass-like residues [13].

Table 3. Comparison of hydraulic resistance values from experimental data with theoretical calculations.

Hydraulic resistance [Pa · s m^{-3}]	PI–PI 3118 × 77 × 22.9 μm	PI–glass 3118 × 77 × 11.6 μm
Theoretical value	4.98×10^{13}	3.44×10^{13}
Experimental value	4.82×10^{13}	1.96×10^{14}

Increasing the chamber pressure in RIE showed increase in the etch rate but at very high pressure the etch rate would tend to decrease again. This is probably due to the fact that by increasing pressure in the chamber the ions can easily be compelled towards the substrate but by increasing it too much the inter collisions of the ions increase and lesser ions hit the surface of the substrate. This was not observed in ICP as pressure above 90 mTorr was not possible in the machine.

Using high power and high pressure to get a higher etch rate is not a viable option, since it was observed that excessive heating of the quartz wafer occurs due to high ion bombardment on the surface of substrate and inappropriate heat dissipation. To etch the higher channels in PI, the surface roughness also plays an important role as explained in [18]. This surface roughness can be controlled either by increasing the fluorine based gas flow [18] or by cleaning the bottom surface of the microfluidic channel by a plasma cleaning step using 50% O_2 and 50% Ar in both RIE and ICP when around few hundreds of nm of PI were left and also by doing BHF dip for 2 min that removes all the left over residues.

The ratio of gases in the mixture is also important for both partially cured and fully cured PI. It was found that the fully cured PI was etched slower with the parameters that were used to etch partially cured PI. The difference in etching rate is due to the fact that in fully cured PI chemical etching is enhanced by the presence of increased fluorine ions which can remove the fully imidized chains, whereas in the partially cured PI, the incomplete chains of PI are easily broken by a lower concentration of fluorine ions.

An alternative approach to the lamination technique demonstrated previously for bonding PI to PI [9, 10, 20] was developed in this paper. The micro fluidic channels were sealed by PI–PI bonding of two partially cured PI layers in the bonding machine, where they were also simultaneously

fully cured. The bonding is strong due to the fact that there are still some chains of PI that are not completely imidized and when they are brought together and cured fully they make the interlayer bond by imidizing across the layers. Leakage and pressure drop measurements have shown the good strength of the bond. The flow rates used for these experiments were chosen as the most commonly used in many POC and biosensor devices. This technique is also simpler to the one previously presented [15], where RF dielectric heating is done by using a high frequency generator to bond two PI layers. The measured pressure drops shown in figure 9 are comparable to those presented in [9]. Depending on the application one can also test how the bonding behaves under harsh conditions like boiling water but this was not tested in this work.

It is also shown that PI processing is a very reliable process in terms of achieved channel height and thickness uniformity over the wafer for the same processing parameters compared to the more commonly used SU8. PI and SU8 are comparable in terms of thickness of the layers achieved but PI has demonstrated better thickness uniformity over the wafer.

5. Conclusion

An easy and fast fabrication process of PI microfluidic devices was developed, which involves dry etching of partially cured PI to form microfluidic channels and PI–PI/glass bonding to make closed channel devices. By this technique the formation of needed integrated microfluidic channels with superior properties in POC and biosensors devices is enabled. These properties include resistance to harsh chemicals and high temperatures, good electrical passivation properties and at the same time better biocompatibility. Moreover, this process is compatible with fabrication of integrated microelectronics circuit that can control the POC and biosensor devices. Hence, it can lead to the development of hand held POC devices with integrated microelectronics and microfluidic channels. In our work we conclude that the best etch rates and etch results are obtained by using the RIE system, where an etch rate of $1.3\,\mu\mathrm{m\,min^{-1}}$ is achieved using power = 100 W, O_2 = 94 sccm, CF_4 = 6 sccm, pressure = 200 mTorr.

Acknowledgments

The authors would like to thank Letizia Amato and Stephan Sylvest Keller for their expert advice on SU8 process and Danchip cleanroom staff for providing all the support for different processes. This project is a part of the EU Marie Curie Initial Training Networks (ITN) Biomedical engineering for cancer and brain disease diagnosis and therapy development: EngCaBra. Project no. PITN-GA-2010–264417.

References

[1] Wu L, Guan G, Hou H W, Bhagat A A S and Han J 2012 Separation of leukocytes from blood using spiral channel with trapezoid cross-section *Anal. Chem.* **84** 9324–31

[2] Agarwal A, Buddharaju K, Lao I, Singh N, Balasubramanian N and Kwong D 2008 Silicon nanowire sensor array using top–down CMOS technology *Sensors Actuators A Phys.* **145–146** 207–13

[3] Rodriguez-Trujillo R, Ajine M A, Orzan A, Mar M D, Larsen F, Clausen C H and Svendsen W E 2014 Label-free protein detection using a microfluidic Coulter-counter device *Sensors Actuators B Chem.* **190** 922–7

[4] Amato L, Keller S S, Heiskanen A, Dimaki M, Emnéus J, Boisen A and Tenje M 2012 Fabrication of high-aspect ratio SU-8 micropillar arrays *Microelectron. Eng.* **98** 483–7

[5] Lee J N, Park C and Whitesides G M 2003 Solvent compatibility of poly(dimethylsiloxane)-based microfluidic devices *Anal. Chem.* **75** 6544–54

[6] Richardson R R, Miller J A and Reichert W M 1993 Polyimides as biomaterials: preliminary biocompatibility testing *Biomaterials* **14** 627–35

[7] Williams K R, Member S, Gupta K, Member S and Wasilik M 2003 Etch rates for micromachining processing—Part II *J. Microelectromech. Sys.* **12** 761–78

[8] Chisca S, Sava I, Musteata V-E and Bruma M 2011 Dielectric and conduction properties of polyimide films *CAS 2011 Proc. of the Int. Semiconductor Conf. (Sinaia, 11–13 October 2010)* pp 253–6

[9] Metz S, Holzer R and Renaud P 2001 Polyimide-based microfluidic devices *Lab Chip* **1** 29–34

[10] Metz S, Bertsch A, Bertrand D and Renaud P 2004 Flexible polyimide probes with microelectrodes and embedded microfluidic channels for simultaneous drug delivery and multi-channel monitoring of bioelectric activity *Biosens. Bioelectron.* **19** 1309–18

[11] Youn S-W, Noguchi T, Takahashi M and Maeda R 2008 Fabrication of micro mold for hot-embossing of polyimide microfluidic platform by using electron beam lithography combined with inductively coupled plasma *Microelectron. Eng.* **85** 918–21

[12] Nguyen T N T and Lee N-E 2007 Deep reactive ion etching of polyimide for microfluidic applications *J. Korean Phys. Soc.* **51** 984

[13] Mimoun B, Pham H T M, Henneken V and Dekker R 2013 Residue-free plasma etching of polyimide coatings for small pitch vias with improved step coverage *J. Vac. Sci. Technol. B Microelectron. Nanom. Struct.* **31** 021201

[14] Bliznetsov V, Manickam A, Chen J and Ranganathan N 2011 High-throughput anisotropic plasma etching of polyimide for MEMS *J. Micromech. Microeng.* **21** 067003

[15] Bayrashev A and Ziaie B 2002 Silicon wafer bonding with an insulator interlayer using RF dielectric heating *Proc. of the 15th IEEE Int. Conf. on MEMS (Las Vegas, NV, 24–25 January 2002)*

[16] Crockett A, Almoustafa M and Vanderlinde W Plasma delayering of integrated circuits (www.triontech.com)

[17] Walewyns T, Scheen G, Tooten E, El Fissi L, Dupuis P and Francis L A 2011 Fabrication of a miniaturized ionization gas sensor with polyimide spacer *Proc. SPIE* **8066** 80660J

[18] Buder U, von Klitzing J-P and Obermeier E 2006 Reactive ion etching for bulk structuring of polyimide *Sensors Actuators A Phys.* **132** 393–9

[19] Richter K, Orfert M and Drescher K 1997 Anisotropic patterning of copper-laminated polyimide foils by plasma etching *Surf. Coat. Technol.* **97** 481–7

[20] Perozziello G *et al* 2012 Microfluidic polyimide chips fabricated by lamination processes for x-ray scattering applications *Proc. of the 16th Int. Conf. on Miniaturized Systems for Chemistry and Life Sciences* pp 686–8